e-Journal of Nondestructive Testing - ISSN 1435-4934 - www.ndt.net

EWSHM 2024
11th European Workshop on Structural Health Monitoring

Birefringent optical fibers to decouple thermo-mechanical effects on FBG sensors

Emanuele CASCIARO [1], Daniela RIGAMONTI[2], Paolo BETTINI[3]
[1] Politecnico di Milano, Milan, Italy, emanuele.casciaro@polimi.it
[2] Politecnico di Milano, Milan, Italy, daniela.rigamonti@polimi.it
[3] Politecnico di Milano, Milan, Italy, paolo.bettini@polimi.it

More info about this article: https://www.ndt.net/?id=29849

Abstract. Fiber Bragg grating (FBG) optical sensors are becoming increasingly important for structural health monitoring (SHM) due to their ability to be integrated into composite materials. A key challenge discussed in the existing literature is the decoupling of thermo-mechanical measurements of these sensors. This study addresses this challenge by using birefringent optical fibers. Birefringent fibers allow an FBG sensor inscribed on them to have two distinct peaks, each responding differently to deformation and temperature changes. This property enables the decoupling of thermo-mechanical measurements by the fiber alone, so that no additional and invasive components are required. The first phase of this work involves the characterization and calibration of an FBG sensor on a birefringent fiber using a dedicated experimental setup. Thermal, mechanical, and thermo-mechanical tests were performed to evaluate the feasibility and effectiveness of the proposed decoupling method. In the subsequent phase, such a sensor was embedded in a composite sample and subjected to the same characterization tests as the single fiber.

Keywords: Fiber Bragg gratings · Fiber optic sensor · Birefringent fiber · Thermo-mechanical decoupling · Composite materials

1. Introduction

This study aims to address the challenge of decoupling thermo-mechanical measurements performed using optical fiber Bragg grating (FBG) inscribed into birefringent optical fibers. These fibers have two polarization axes, resulting in two sensor peaks at different wavelengths that respond differently to thermal and mechanical changes. The method involves monitoring the evolution of the peak wavelengths after calibrating the sensor. The advantage of this technique is the ability to decouple thermal measurements from mechanical ones at the same measurement point without the need for additional components. The research comprises two main phases: the first focuses on the characterization of a single birefringent fiber with an FBG sensor through tests involving temperature variations only, axial deformations only, and mixed tests with deformation and temperature variations. In the second phase, the same sensor is characterized when embedded in a composite sample. The

This work is licensed under CC BY 4.0

Media and Publishing Partner
https://doi.org/10.58286/29849

same tests will be performed to compare the response of the sensor. Two experimental setups are used for the experimental tests: one developed for testing the non-embedded fiber, and another, for the composite sample, which requires the use of a furnace and a Materials Test System (MTS). The paper is structured as follows: section 2 discusses the state of the art and applications of birefringence fibers. Section 3 describes the design of the test system developed for the analysis of the non-embedded fiber. Section 4 discusses the characterization of fibers and mixed tests, while Section 5 describes the production of composite specimens, the setup used, the characterization tests and the mixed tests. Section 6 deals with conclusions and future developments.

2. State of the Art

Structural Health Monitoring (SHM) is a critical focus in the aerospace industry, encompassing tools and techniques for monitoring structural integrity. FBG sensors are highly regarded due to their lightweight design, compact size, embeddability in composites, and resistance to electromagnetic interference. This study places particular emphasis on birefringent fibers, which divide incident light into two distinct rays. In polarization-maintaining (PM) or birefringent optical fibers, these rays travel at different speeds along the slow and fast axes. Birefringence in optical fibers can be induced through methods like Shape-Induced Birefringence or Stress-Induced Birefringence [1], as in this work. Birefringent optical fibers have undergone extensive examination to assess their effectiveness as sensors in various setups, including local and integral measurement systems. Notably, the utilization of a Sagnac interferometer in integral systems yielded impressive results in terms of decoupling [2]. This study utilizes segments of birefringent fibers, joined with appropriately phased principal polarization axes. It was possible to achieve accurate measurements with relative errors of approximately ±3 $\mu\varepsilon$ and ±0.4 ℃. In another study, Zhou et al. [3] employed a FBG connected in series to a segment of birefringent optical fiber, reporting measurement errors 1 ℃ and 21 $\mu\varepsilon$. Qazi et al. [4] demonstrated promising results with a configuration involving a D-shaped cross-sectional area of the fiber, achieving sensitivities of 46 $pm/\mu\varepsilon$ and 130 $pm/$℃ for a limited range of strains and temperatures (from 0 to 50 $\mu\varepsilon$ and from 30 ℃ to 80 ℃). The work of Ferreira et al. [5] explored the use of bow-tie birefringent fibers to distinguish signals from slow and fast axes. The article focuses on describing the results obtained with errors of approximately ±1.3 ℃ and ±13.5 $\mu\varepsilon$. Cross-tests were also performed and have yielded promising results. Lastly, Zhang et al. [6] presented an integral measurement system utilizing a distributed sensor on birefringent fiber for measuring pressure along its entire length. The system demonstrated accurate decoupling of pressure and temperature with an accuracy of 0.014 ℃ and 0.15 bar. In the category of sensors capable of making point measurements while decoupling the thermo-mechanical effects, we can refer to the work of J. Van Roosbroeck et al. that explored the use of a Bragg grating sensor inscribed in a PM fiber [7]. Thermo-mechanical decoupling was verified with a temperature variation of approximately ±0.2 ℃, employing the difference between the two peaks for temperature measurements and the wavelengths of the sensors for deformation measurements. A. K. Singh et al. [8] proposed an innovative approach using a standard optical fiber (SMF) embedded in a composite laminate to induce birefringence. The parameters investigated are the Bragg wavelength and the sensor bandwidth. The errors for the strain and temperature measurements were found to be 62 $\mu\varepsilon$ and 1.94 ℃. Numerical investigation by Andrea Annunziato et al. simulated the presence of birefringent optical fibers embedded in a composite material [9]. They found variations in temperature sensitivity due to different fibers and embedding techniques, with Bow-Tie fiber exhibiting the best performance in strain and temperature decoupling.

3. Measurement System

Unprotected optical fibers are susceptible to damage when loaded perpendicular to their axis, requiring careful handling. This fragility underscores the importance of using appropriate instruments (figure 1(a)), capable of measuring wavelength variations due to axial deformations, temperature variations, or both simultaneously without damaging the fiber.

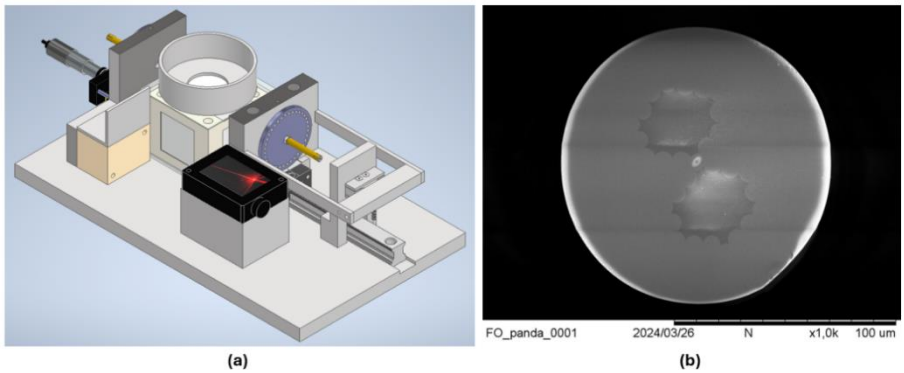

Fig. 1. Experimental setup (a), SEM section of the PM Panda fiber (b)

The primary components of the system are the fastening mechanisms for optical fibers, comprising two brass "chucks" that secure the fiber with a threaded ring and precise clamping force. One chuck is attached to a micrometric slide for controlled movement, while the other is on a carriage with linear ball guides. The tension force applied to the fiber by the micrometric slide causes movement within the structure connected to the second chuck, exerting force on a load cell, which indicates the force applied to the fiber. Adjustments were made to refine force measurement and mitigate friction effects during assembly. In the central section, an insulated cube allows the fiber to pass without contact and accommodates a heating plate, employing the Joule effect, to uniformly heat the environment and to control the temperature. This part is enclosed by a plexiglass cover for thermal insulation and transparency. Symmetrical grooves in the cover guide the fiber, with a cutout for a cooling system and holes for cable routing. A laser sensor integrated with the micrometric slide detects fiber deformation. The polarization-maintaining fiber is connected to a polarization controller consisting of quarter-wave and half-wave plates, allowing precise phase shifts to control light polarization, thus the intensity of the two peaks from the Bragg grating. At the exit from the controller, the fiber is connected to a dynamic optical interrogation system (SM130 produced by Micron Optics).

4. Thermo-mechanical characterization of the fiber

The investigated Panda polarization-maintaining fiber (figure 1(b)) has a cladding diameter of 125 μm and is coated with Ormocer. An FBG sensor of 8 mm was inscribed using FBGS's Draw Tower Gratings (DTG) technology. The temperature sensitivity of the sensor was calibrated using the test system described above. The temperature range selected for the characterization ranged from 30 ℃ to 90 ℃. For each test, the fiber was first heated to 90 ℃ in 10 ℃ increments and then cooled down using the same method. Three tests were carried out for each heating and cooling ramp.

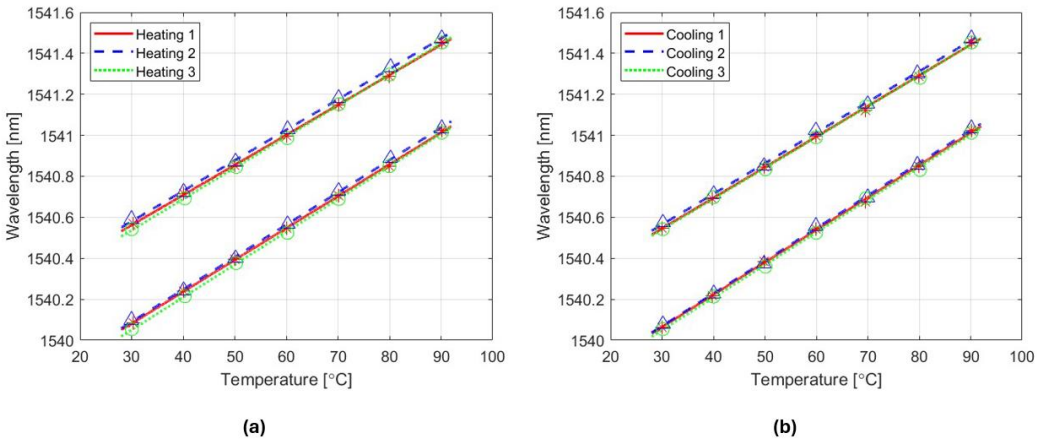

Fig. 2. FBGS wavelengths in PM fiber in insulated fiber during heating (a) and cooling (b)

The analyses show that the distance between the peaks decreases during heating (figure 2). This effect is attributed to the change in the birefringence of the fibre with temperature. During the three tests, the curves are linear and overlap, which underlines the repeatability of the measurements. The temperature sensitivities are $K_{T1} = 0.01581237\ nm/°C$ and $K_{T2} = 0.01494327\ nm/°C$ for the fast axis and the slow axis respectively. The next step was to carry out tests at ambient temperature with different levels of strain. The deformation was applied in steps, starting from 0 mm and increasing to 1.1 mm in steps of 0.1 mm. The ramp was first run in the upward direction and then in the downward direction. The elongation was achieved by rotating the screw on the micrometer slide. A maximum elongation of 1.1 mm was chosen to prevent potential damage to the fiber. During each step, in addition to recording the wavelengths, the force exerted by the stretched fiber on the load cell and the signal from the laser sensor were also recorded.

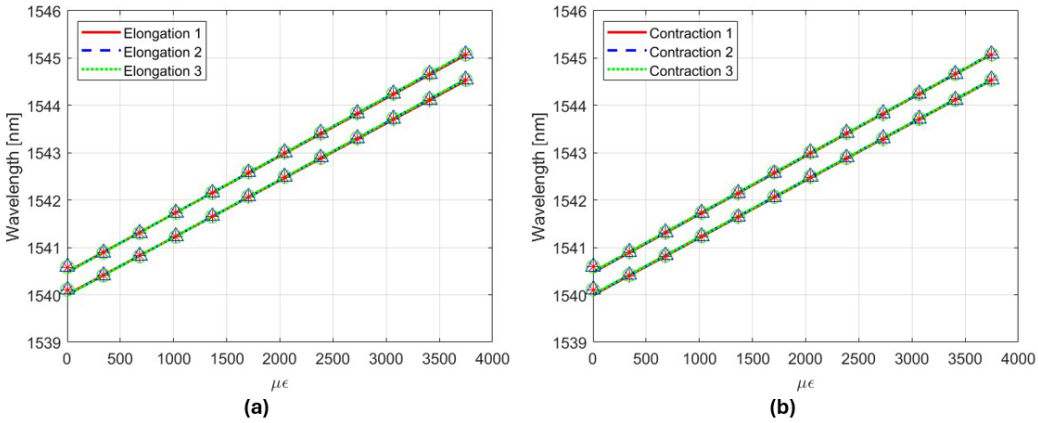

Fig. 3. FBGS wavelength in PM fiber in insulated fiber as axial load increases (a) and decreases (b)

The response of the sensor remains linear (figure 3). The repeatability of the measurement is ensured by the overlapping of the data. The sensitivities obtained for the axial strain are $K_{\varepsilon 1} = 0.00121107\ nm/\mu\varepsilon$ and $K_{\varepsilon 2} = 0.001228522\ nm/\mu\varepsilon$ for the fast and slow axis respectively. It is worth noting that while the peaks diverge slightly in the mechanical characterization tests, they tend to converge in the thermal characterization tests. However, the temperature sensitivities of both axes are one order of magnitude greater than the strain sensitivities. This indicates that the phenomena do not cancel each other out and that thermo-mechanical decoupling is possible. The concluding step of this initial experimental phase entails testing the response of the optical fiber to simultaneous variations in temperature and strain. It is divided into two parts: constant temperature (variable strain) and constant strain (variable temperature). In the first case, at constant temperature, a ramp of increasing and decreasing axial strain is performed. In the second case, a constant strain is

applied and a thermal ramp is performed. For these mixed tests, the sensitivities derived from the previous calibration phase were used, but the results were not satisfactory. This phenomenon is thought to be due to the dependence of the refractive index on the wavelength. It was therefore decided to carry out a further calibration phase directly with the mixed tests, varying the deformation at different temperatures. The system of equations related to the two peaks of the FBGS was constituted by axial strain sensitivities, from the mixed tests, together with the temperature sensitivities obtained from the zero deformation tests. So, the calibration of the sensor was conducted during constant deformation tests as the temperature changed. The same experimental setup as described in section 3 was used. A temperature ramp from 10 °C to 80 °C was performed, with 10 °C steps. For each of these 8 temperatures, a deformation ramp was performed in steps of 0.1 mm from 0 mm to 1.1 mm in both ascending and descending directions. The sensitivity to axial deformation at different temperatures was determined from the calibration curves (figure 4(a)).

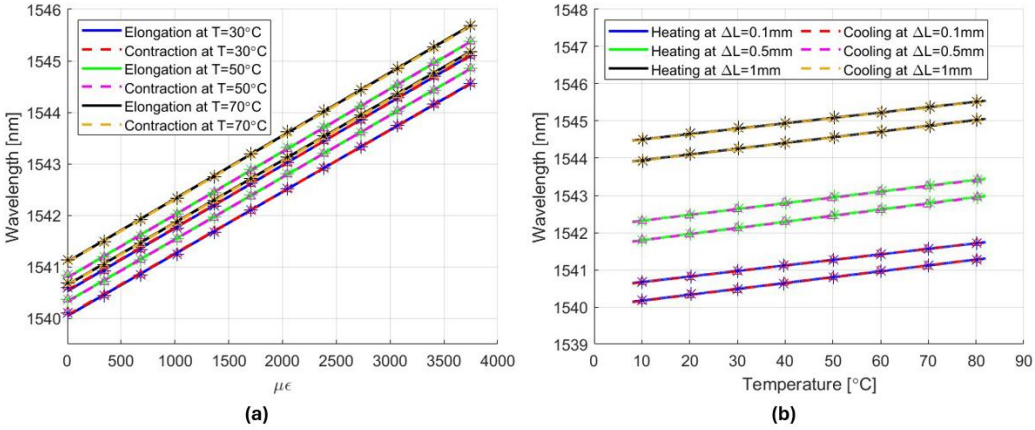

Fig. 4. Calibration curves as the deformation varies at constant temperature (a), wavelengths within the temperature range at constant strain (where ΔL represents the elongation imposed on the fiber) (b)

For the constant deformation and temperature variation tests, in each 0.1 mm increment, ranging from 0 mm to 1.1 mm, the temperature was systematically increased from 10 °C to 80 °C (in 10 °C intervals) and then decreased in the same manner. The wavelength changes observed at the different temperatures show linearity with constant deformation (figure 4(b)). The relative slope between the fast and slow axis lines is consistent with what was observed in the thermal characterization tests of the fiber under zero strain conditions. This confirms the chosen approach where we employ the axial deformation sensitivities from the previous mixed calibration tests while relying on the temperature sensitivities calculated during the initial phase at zero deformation. It was possible to invert the resolution system and check that the trend of the variables measured by the FBG sensor matched that of the thermocouple and the displacement transducer.

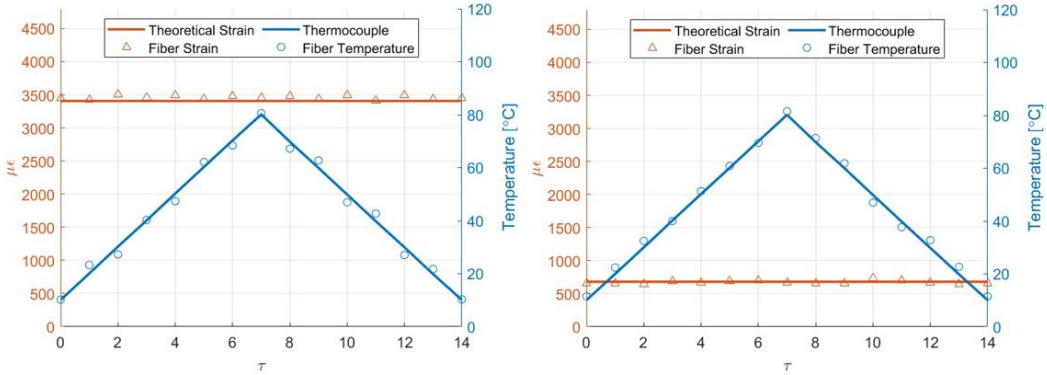

Fig. 5. Difference between deformation and temperature calculated with the FBG sensor in PM fiber and the known values from the micrometer slide and thermocouple

Figure 5 shows the heating and cooling ramps, which specify an elongation of 1 mm and 0.2 mm respectively. The temperature trend is accurately recorded by the fiber, with an error margin of ±3 ℃. The strain measurement is even more precise and ensures a margin of error of ±50 $\mu\varepsilon$. These results demonstrate the effectiveness of the calibration process. Importantly, the trends of temperature and strain are completely independent, allowing thermo-mechanical decoupling with PM fiber.

5. Thermo-mechanical characterization of the fiber in composite specimens

After characterizing the isolated fiber, we proceeded to characterize the behavior of a composite material component in which the optical fiber sensor was embedded (figure 6). The material used consisted of twelve layers of a prepreg made of unidirectional glass fibers (Solvay, CYCOM 5216). The optical fiber was embedded after three layers of prepreg from the mold.

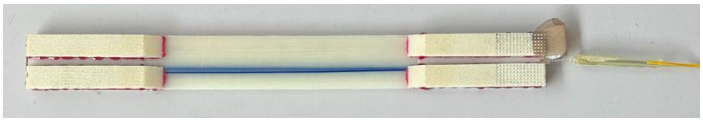

Fig. 6. Composite specimen with PM fiber embedded, equipped with FBG sensor

The tests performed on the sample were similar to those performed on the individual fiber, but with a different setup due to the nature of the component itself. In the first experiments, the deformation was set to zero while the temperature was varied. The sample was positioned in a Mazzali s.n.c. Thermotest A505E1 oven and a thermocouple was placed near the sensor. To ensure repeatability, each experiment was performed three times.

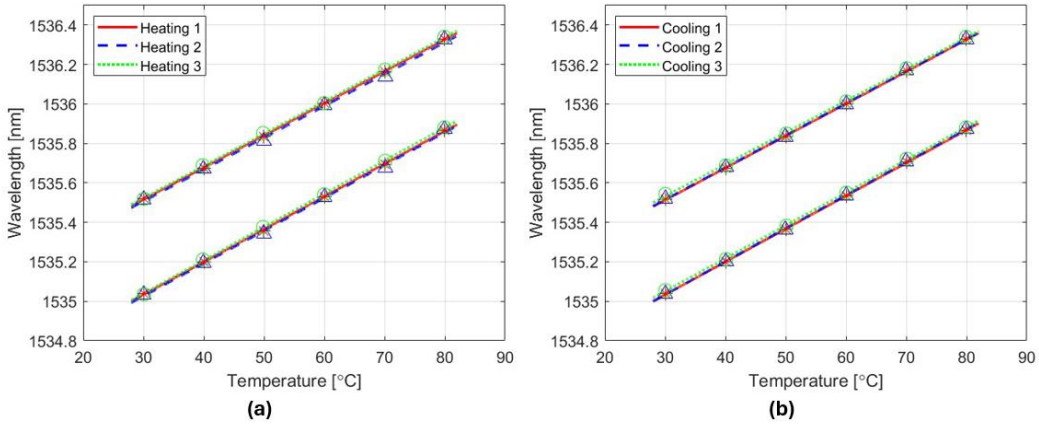

Fig. 7. FBGS wavelengths in PM fiber in the composite specimen during heating (a) and cooling (b)

It can be stated that the trend within the temperature range exhibits perfect linearity (figure 7). The almost identical slopes and overlapping lines ensure the repeatability. Similar to the isolated fiber, it is noticeable that the lines tend to converge as temperature increases. The average temperature sensitivities for both the fast and slow axes are $K_{T1} = 0.01669775\ nm/℃$ and $K_{T2} = 0.01621977\ nm/℃$. The next step was to test the behavior of the sample under different strains. The setup used consisted of a Materials Test System (MTS) designed for axial deformation tests, in which the composite sample was clamped and equipped with an extensometer. The strain, in the MTS, is obtained by force. It was decided to perform a deformation ramp by applying a force from 0 N to 10000 N in steps of 1000 N and vice versa. The experiment was repeated three times to ensure repeatability.

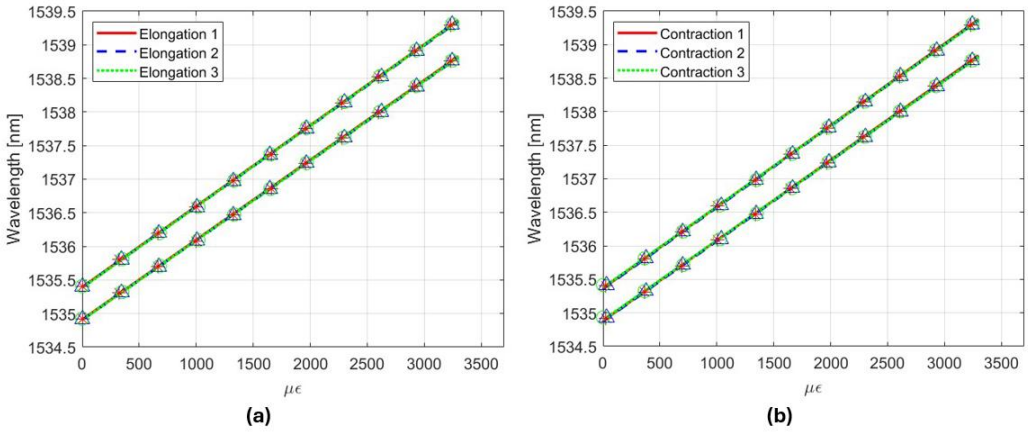

Fig. 8. FBGS wavelength in PM fiber in the composite specimen as axial load increases (a) and decreases (b)

In the considered range of axial strain, the trend of the curves is perfectly linear (figure 8). The uniform slope and overlap of the lines ensure the experiment's repeatability. It's worth noting that the lines are not perfectly parallel; rather, they tend to diverge. The difference in relative displacement between the peaks is less pronounced when discussing deformations compared to temperature, by an order of magnitude. The average strain sensitivities of the fast and slow axes were $K_{\varepsilon 1} = 0.001191136\ nm/\mu\varepsilon$ and $K_{\varepsilon 2} = 0.001208293\ nm/\mu\varepsilon$, respectively. Upon completion of the sensitivity calculations, thermo-mechanical characterization tests were conducted. The tests were categorized into two groups: tests maintaining constant strain (varying temperature) and tests maintaining constant temperature (varying strain). Continuous mode wavelength acquisition was chosen. The specimen was affixed to the MTS tensile testing machine and outfitted with an extensometer and a thermocouple. A pair of infrared lamps was used. Their placement was optimized to ensure uniform heat distribution across the specimen. Upon completion of data acquisition from the constant strain tests (varying temperature), sensor calibration was conducted similarly to the procedure followed for the isolated fiber, considering the variation of the refractive index with wavelength. For the experimental validation tests, namely those conducted at constant temperature, the setup mirrored that of the tests involving constant strain and variable temperature. The lamps were positioned at a defined distance from the specimen to increase its temperature until it reached a steady-state condition. Subsequently, the desired deformation was imparted utilizing the MTS machine. The deformation ramp employed was the same as in the previous tests.

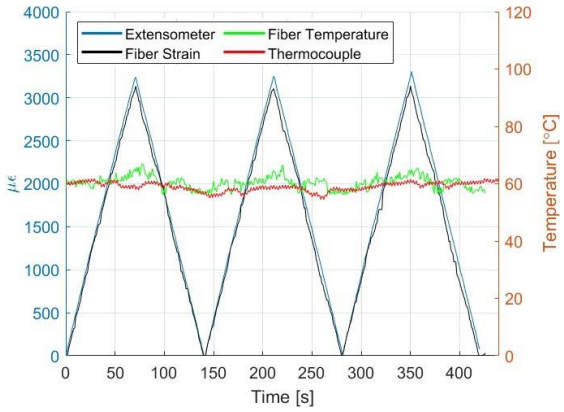

Fig. 9. Mixed test with constant temperature and varying strain

The calculated strain values from the fiber closely track the trend of the data acquired through the extensometer, with minimal errors on the order of ±150 $\mu\varepsilon$. Moreover, the temperature measured by the fiber accurately mirrors the trend of the data provided by the

thermocouple, with errors of about ±5 ℃. A slight coupling effect is observed in figure 9, where the temperature follows the strain trend. Nevertheless, these results are considered satisfactory and serve as a starting point for future studies.

6. Conclusions and future developments

The research conducted focuses on developing a sensor capable of decoupling thermo-mechanical effects. Initially, the performance of an FBG sensor in a birefringent optical fiber was investigated, requiring mixed tests for calibration due to refractive index variation. Temperature measurements showed a ±3 ℃ error, while strain measurements had a ±50 $\mu\varepsilon$ error. Subsequently, the sensor was integrated into a composite material specimen, showing temperature errors within ±5 ℃ and strain errors of ±150 $\mu\varepsilon$. This confirms the feasibility of embedding birefringent fibers into composite structures for monitoring temperature and deformation variations without additional components. It's crucial to note that sensor sensitivities change when embedded in the composite, necessitating recalibration for each new structure. Future research may explore the sensor's behavior across wider temperature ranges and investigate configurations to avoid ill-conditioned systems.

Acknowledgements

This work has been carried out with Dr. M. Griffanti and Dr. F. Crepaldi. This research has been supported by ASI (Italian Space Agency), grant agreement 2018-5-HH.0.

References

[1] R. Guan, F. Zhu, Z. Gan, D. Huang, and S. Liu, “Stress birefringence analysis of polarization maintaining optical fibers”, *Optical Fiber Technology*, vol. 11, no. 3, pp. 240–254, 2005, doi: 10.1016/j.yofte.2004.10.002.

[2] G. Sun, H. Tang, Y. Hu, and Y. Zhou, “Strain and temperature discrimination using high birefringence fiber Sagnac interferometer with enhanced sensitivities”, *IEEE Photonics Technology Letters*, vol. 24, no. 7, pp. 587–589, 2012, doi: 10.1109/LPT.2012.2184087.

[3] D. P. Zhou, L. Wei, W. K. Liu, and J. W. Y. Lit, “Simultaneous measurement of strain and temperature based on a fiber Bragg grating combined with a high-birefringence fiber loop mirror”, *Opt Commun*, vol. 281, no. 18, pp. 4640–4643, Sep. 2008, doi: 10.1016/j.optcom.2008.06.001.

[4] H. H. Qazi, A. B. Mohammad, H. Ahmad, and M. Z. Zulkifli, “D-shaped polarization maintaining fiber sensor for strain and temperature monitoring”, *Sensors (Switzerland)*, vol. 16, no. 9, Sep. 2016, doi: 10.3390/s16091505.

[5] L. A. Ferreira, F. M. Araú, J. L. Santos, and F. Farahi, “Simultaneous measurement of strain and temperature using interferometrically interrogated fiber Bragg grating sensors”, *Optical Engineering*, vol. 39, issue 9, August 2000, https://doi.org/10.1117/1.1305493.

[6] L. Zhang *et al.*, “Long-distance distributed pressure sensing based on frequency-scanned phase-sensitive optical time-domain reflectometry”, *Opt Express*, vol. 29, no. 13, p. 20487, Jun. 2021, doi: 10.1364/oe.425501.

[7] J. Van Roosbroeck, S. K. Ibrahim, E. Lindner, K. Schuster, and J. Vlekken, “Stretching the limits for the decoupling of strain and temperature with FBG based sensors”, in *24th International Conference on Optical Fibre Sensors*, SPIE, Sep. 2015, p. 96343S. https://doi.org/10.1117/12.2194806, date of access: 2024-05-17.

[8] A. K. Singh, S. Berggren, Y. Zhu, M. Han, and H. Huang, “Simultaneous strain and temperature measurement using a single fiber Bragg grating embedded in a composite laminate”, *Smart Materials and Structures*, vol. 26, no. 11, p. 115025, October 2017, doi: 10.1088/1361-665X/aa91ab.

[9] A. Annunziato, F. Anelli, J. Gates, C. Holmes, and F. Prudenzano, “Design of Polarization-Maintaining FBGs Using Polyimide Films to Improve Strain-Temperature Sensing in CFRP Laminates”, *IEEE Photonics J*, vol. 13, no. 2, Apr. 2021, doi: 10.1109/JPHOT.2021.3063172.